Acta Crystallographica Section C
Crystal Structure Communications
ISSN 0108-2701

N-Z-Pro–D-Leu using synchrotron radiation data from a very small crystal

Henrik Birkedal,* Dieter Schwarzenbach and Philip Pattison

Institute of Crystallography, University of Lausanne, BSP, Dorigny, CH-1015 Lausanne, Switzerland
Correspondence e-mail: henrik.birkedal@ic.unil.ch

Received 19 October 2000
Accepted 16 May 2001

The crystal structure of the neuroactive artificial dipeptide *N*-benzyloxycarbonylprolyl-D-leucine, $C_{19}H_{26}N_2O_5$, was solved using synchrotron radiation data collected on a very small crystal ($20 \times 20 \times 380\ \mu$m). The molecules form hydrogen-bonded 2_1 helices. The acid carbonyl group does not participate in strong hydrogen bonds. This is interpreted as a consequence of close-packing requirements.

Comment

N-Benzyloxycarbonylprolyl-D-leucine (NZPL) is a synthetic dipeptide protected on the N-terminal side by a benzyloxycarbonyl (Z) group. The compound is effective as an inhibitor of the development of tolerance to and physical dependence on morphine in mice (Walter *et al.*, 1978, 1979). It appears to influence the brain stem concentration of norandrenaline and dopamine (Kovács *et al.*, 1981, 1983, 1984), showing that its function is linked to the neurotransmitter system of the brain. Furthermore, Szabó *et al.* (1987) found that NZPL attenuates the development of tolerance to the hypothermic effect of ethanol.

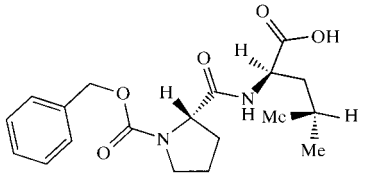

NZPL

Here, we present the crystal structure of NZPL solved using synchrotron radiation data collected at the Swiss–Norwegian Beam Line (SNBL) at the European Synchrotron Radiation Facility, France. SNBL is situated at a bending magnet. A MAR345 imaging plate system and focusing optics were employed for the measurements. The crystal was very small and measured only $20 \times 20 \times 380\ \mu$m. Despite this small size, data of satisfactory quality could be collected and the structure solved and refined; see the refinement statistics.

The molecular backbone is bent at C2*A* and φ_2 is 112.6 (3)° (see Fig. 1). The Pro residue adopts an envelope conformation; C1*G* is in the N1*A*—C1*A*—C1*D* plane [Δ = −0.001 (11) Å], while C1*B* is 0.540 (9) Å below it. This is also reflected in the torsion angles (Table 1). There appears to be somewhat reduced delocalization over the peptide bond between Z and Pro, as seen by comparing the bond lengths (C═O and C—N) with those of the delocalized peptide link between Pro and D-Leu.

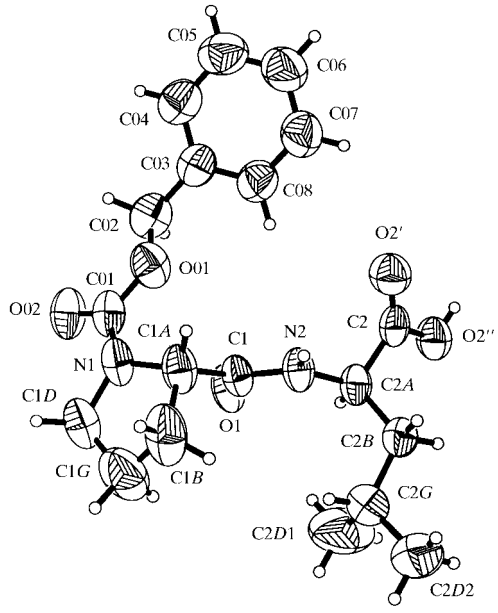

Figure 1
The molecular structure and labeling scheme of NZPL. Displacement ellipsoids are drawn at the 50% probability level.

The most interesting feature of the present structure is the imbalance between the number of donors and acceptors of classical hydrogen bonds. There are three hydrogen-bond acceptors (O02, O1 and O2′) but only two strong donors (O2″—H2″ and N2—H2). Surprisingly, the structure does not form carboxylic acid dimers. O2′ does not accept any classical hydrogen bonds; see Table 2. The carboxylic acid moiety is a donor in an O—H···O hydrogen bond with O1^{i}. Together with the remaining strong hydrogen bonds (Table 2), this leads to helical 2_1 columns along the *a* axis, as illustrated in Fig. 2. Further stabilization of this columnar structure is provided by C—H···O contacts (Table 2). One of these is to O2′, while the second is to O1. The latter is the shortest, as would be expected from the slightly higher acidity of CO2 compared with C2*B*. In addition to these intermolecular contacts, there is a very short intramolecular C—H···O contact (C2*A*—H2*A*···O1), making a C_5 ring. It is unclear whether this interaction is attractive or not. The fact that carboxylic acid dimers or catamers do not form and that the acid carbonyl oxygen does not accept strong hydrogen bonds is certainly due to close-packing requirements and the hydrogen-bond donor–acceptor imbalance. This demonstrates that close-packing is a principal factor governing crystal structures.

The study of small crystals using synchrotron radiation has been reviewed by Harding (1988, 1995, 1996), Rieck & Schulz (1991), Clegg (2000) and Birkedal (2000). Two measures of scattering powers have been proposed. Rieck *et al.* (1988) suggest using $S = [F(000)/V_{cell}]^2 V_{crystal}\lambda^3$, while Harding (1988)

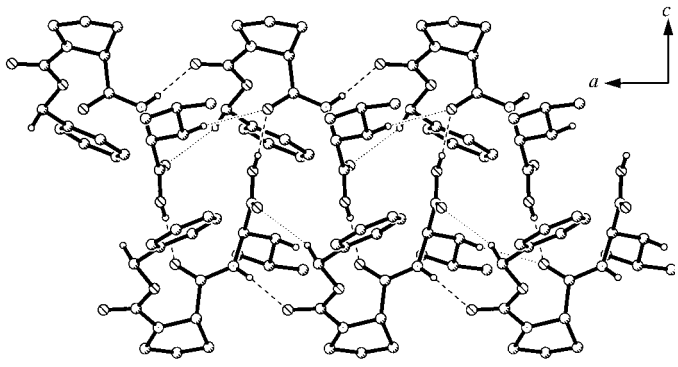

Figure 2
The helical hydrogen-bonded column in NZPL projected along the *b* axis. Dashed lines indicate N—H···O and O—H···O hydrogen bonds, while dotted lines represent C—H···O close contacts.

used $S' = V_{crystal}(\Sigma f_i^2/V_{primitive}^2)$, where $V_{crystal}$ is the sample volume, $V_{primitive}$ is the volume of the primitive unit cell and Σf_i^2 is the sum of the squares of the atomic numbers over the primitive unit cell. With these definitions we get $S = 1.2 \times 10^{16}$ e^2 and $S' = 1.7 \times 10^{14}$ e^2 Å^{-3}. These scattering powers lie between those accessible with laboratory equipment and those requiring dedicated microfocus beam lines. They are of the same order of magnitude as those considered to belong to the class of very small crystals by Harding (1996). The present data set extends to 0.9 Å and as many as 88% of the measured reflections are observed at the $I > 2\sigma(I)$ level. This exceeds the typical qualities quoted by Harding (1996). Note that the present sample is needle-shaped. Clearly, it is the smallest dimension that effectively defines a crystal to be of micro size. A cube-shaped sample with side lengths of 20 μm yielding scattering powers $S = 3.2 \times 10^{14}$ e^2 and $S' = 9.1 \times 10^{12}$ e^2 Å^{-3}, which is typical of the microcrystal domain (Birkedal, 2000), could have been measured with the installation of SNBL. In the present experiment, the exposure time was 5 s per image. This resulted in several saturated low-order reflections and a second data set was collected with an attenuating filter in the incident beam. To measure a crystal of 20 times smaller volume would thus correspond to an exposure time of 100 s per image. This would have increased the measuring time from 130 min to only 270 min for a complete data set of high quality. This small increase in measuring time reflects the fact that a large part of the experiment time is used for detector read out (Birkedal, 2000). These considerations demonstrate that the present setup would be quite capable of measuring purely organic samples in the 20 × 20 × 20 μm range. This result opens up some interesting experimental possibilities on bending-magnet beamlines at third generation synchrotrons for microcrystal diffraction, hitherto considered to be an exclusive domain of dedicated insertion-device beamlines.

Experimental

A single crystal was selected directly from the commercially acquired batch (Sigma C4644, lot 23 F5900) and mounted on a thin glass needle. The size was estimated from optical microscopy images at 80 × magnification. The s.u.'s given in the *Crystal data* table reflect our estimated confidence in these numbers. Two data collections were performed: HIGH and LOW. Dataset HIGH was performed with a crystal-to-detector distance of 130 mm and a 5 s exposure time. Data set LOW was performed with a 50 μm Cu-filter in the beam, a crystal-to-detector distance of 180 mm and a 20 s exposure time. This second data set was collected to compensate for the limited dynamic range of the detector and effectively corresponds to a measurement of the strong low-order reflections. For both data sets, 90 images were collected. A 2° oscillation range was used for all images, which roughly corresponds to a hemisphere of data. Before the data collection started, we verified on a test image that none of the symmetry elements of the crystal were parallel to the oscillation axis to ensure as complete a data set as possible. The final data set was more than 96% complete. The beam size, selected with the MAR345 receiving slits, was 0.5 × 0.5 mm. The degree of linear polarization was assumed to be 0.96. This value was found to be valid for the present set-up under similar experimental conditions (Birkedal, 2000). The mosaic spread of the crystal was somewhat non-uniform and orientation dependent. The chosen peak shape is a compromise between the small spot sizes found on some images and the larger ones found on others. The data were corrected for changes in the incident beam intensity by an interframe scaling procedure as implemented in *SCALEPACK* (Otwinowski & Minor, 1997). By comparing the scale factors of individual frames of data set HIGH with the corresponding ones of LOW, we determined the effective attenuation factor of the incident-beam Cu absorber foil to be 17.9 (3).

Crystal data

$C_{19}H_{26}N_2O_5$	Synchrotron radiation
M_r = 362.42	λ = 0.8008 Å
Orthorhombic, $P2_12_12_1$	Cell parameters from 6811 reflections
a = 6.8870 (14) Å	θ = 2.0–26.4°
b = 12.851 (3) Å	μ = 0.09 mm^{-1}
c = 22.462 (5) Å	T = 293 (2) K
V = 1988.0 (7) Å^3	Needle, colourless
Z = 4	0.380 (5) × 0.020 (3) × 0.02 (3) mm
D_x = 1.211 Mg m^{-3}	

Data collection

MAR345 diffractometer	R_{int} = 0.045
φ scans	θ_{max} = 26.4°
11028 measured reflections	$h = -7 \rightarrow 7$
1613 independent reflections	$k = -14 \rightarrow 14$
1413 reflections with $I > 2\sigma(I)$	$l = -24 \rightarrow 24$

Table 1
Selected geometric parameters (Å, °).

O01—C02	1.445 (4)	C1—N2	1.333 (3)
O02—C01	1.227 (4)	O2′—C2	1.197 (4)
C01—N1	1.345 (4)	O2″—C2	1.328 (3)
O1—C1	1.240 (3)	N2—C2*A*	1.444 (4)
N1—C1*A*	1.466 (4)	C2—C2*A*	1.514 (5)
C1*A*—C1	1.514 (4)		
O01—C01—N1—C1*A*	−18.2 (4)	C1*A*—N1—C1*D*—C1*G*	0.0 (4)
C01—N1—C1*A*—C1	−60.3 (5)	C1*A*—C1—N2—C2*A*	169.9 (3)
N1—C1*A*—C1—N2	167.3 (3)	C1—N2—C2*A*—C2	112.6 (3)
N1—C1*A*—C1*B*—C1*G*	33.7 (4)	O2′—C2—C2*A*—N2	16.3 (4)
C1—C1*A*—C1*B*—C1*G*	−84.1 (4)	O2″—C2—C2*A*—N2	−165.5 (2)
C1*A*—C1*B*—C1*G*—C1*D*	−35.1 (5)		

Refinement

Refinement on F^2	$w = 1/[\sigma^2(F_o^2) + (0.0549P)^2 + 0.2963P]$ where $P = (F_o^2 + 2F_c^2)/3$
$R[F^2 > 2\sigma(F^2)] = 0.036$	$(\Delta/\sigma)_{max} < 0.001$
$wR(F^2) = 0.104$	$\Delta\rho_{max} = 0.11$ e Å^{-3}
$S = 1.05$	$\Delta\rho_{min} = -0.10$ e Å^{-3}
1613 reflections	Absolute structure: fixed by known peptide configuration
238 parameters	
H-atom parameters constrained	

Table 2
Hydrogen-bonding geometry and close C—H···O contacts (Å, °).

D—H···A	D—H	H···A	D···A	D—H···A
O2′′—H2′′···O1^{i}	0.82	1.88	2.655 (3)	158
N2—H2···O02^{ii}	0.86	2.07	2.920 (3)	172
C2*B*—H2*B*2···O1^{ii}	0.97	2.52	3.438 (4)	157
C02—H02*B*···O2′^{iii}	0.97	2.57	3.486 (4)	158
C2*A*—H2*A*···O1	0.98	2.37	2.798 (3)	106

Symmetry codes: (i) $x-\frac{1}{2}, \frac{3}{2}-y, -z$; (ii) $x-1, y, z$; (iii) $1+x, y, z$.

Due to the lack of chiral resolving power in the experiment (no sizeable anomalous scattering contribution), Friedel mates were averaged. The enantiomer was chosen so that the peptide had the known chirality.

Cell refinement: *HKL* (Otwinowski & Minor, 1997); data reduction: *HKL*; program(s) used to solve structure: *SHELXS*97 (Sheldrick, 1997); program(s) used to refine structure: *SHELXL*97 (Sheldrick, 1997); molecular graphics: *XP* (Siemens, 1996).

We thank the staff of the Swiss–Norwegian Beam Line for their kind support and the Swiss National Science Foundation for funding. HB thanks the Danish Research Agency for additional financial support.

Supplementary data for this paper are available from the IUCr electronic archives (Reference: SX1122). Services for accessing these data are described at the back of the journal.

References

Birkedal, H. (2000). PhD thesis, University of Lausanne, Switzerland.
Clegg, W. (2000). *J. Chem. Soc. Dalton Trans.* pp. 3223–3232.
Harding, M. M. (1988). *Chemical Crystallography with Pulsed Neutrons and Synchrotron X-rays*, edited by M. A. Carrondo & G. A. Jeffrey, pp. 537–561. NATO ASI Vol. C221. Dordrecht: D. Reidel Publishing Company.
Harding, M. M. (1995). *Acta Cryst.* B**51**, 432–446.
Harding, M. M. (1996). *J. Synchrotron Rad.* **3**, 250–259.
Kovács, G. L., Acsai, L., Tihanyi, A., Faludi, M. & Telegdy, G. (1983). *Pharmacol. Biochem. Behav.* **18**, 345–349.
Kovács, G. L., Szontágh, L., Baláspiri, L., Hódi, K., Bohus, P. & Telegdy, G. (1981). *Neuropharmacology*, **20**, 647–651.
Kovács, G. L., Telegdy, G. & Hódi, K. (1984). *Pharmacol. Biochem. Behav.* **21**, 345–348.
Otwinowski, Z. & Minor, W. (1997). *Methods Enzymol.* **276**, 307–326.
Rieck, W., Euler, H. & Schulz, H. (1988). *Acta Cryst.* A**44**, 1099–1101.
Rieck, W. & Schulz, H. (1991). *Handbook on Synchrotron Radiation*, Vol. 3, edited by G. Brown & D. E. Moncton, pp. 267–290. Amsterdam: Elsevier Science Publishers BV.
Sheldrick, G. M. (1997). *SHELXS*97 and *SHELXL*97. University of Göttingen, Germany.
Siemens (1996). *XP*. Version 5.04. Siemens Analytical X-ray Instruments Inc., Madison, Wisconsin, USA.
Szabó, G., Kovács, G. L., Székeli, S., Baláspri, L. & Telegdy, G. (1987). *Acta Phys. Hung.* **69**, 115–122.
Walter, R., Ritzmann, R. F., Bhargava, H. N. & Flexner, L. B. (1979). *Proc. Natl Acad. Sci. USA*, **76**, 518–520.
Walter, R., Ritzmann, R. F., Bhargava, H. N., Rainbow, T. C., Flexner, L. B. & Krivoy, W. A. (1978). *Proc. Natl Acad. Sci. USA*, **75**, 4573–4576.